PHYSICAL REVIEW E, VOLUME 63, 035304(R)

Symmetry breaking, anomalous scaling, and large-scale flow generation in a convection cell

Ananias G. Tomboulides* and Victor Yakhot
Department of Aerospace and Mechanical Engineering, Boston University, 110 Cummington Street, Boston, Massachusetts 02215
(Received 5 October 2000; published 20 February 2001)

We consider a convection process in thin loops of different geometries. At $\mathrm{Ra}=\mathrm{Ra}'_{cr}$ a first transition leading to the generation of corner vortices is observed. At higher Ra ($\mathrm{Ra}>\mathrm{Ra}_{cr}$) a coherent large-scale flow, which persists for a very long time, sets up. The mean velocity $\overline{v}$, mass flux $\dot{m}$, and the Nusselt number Nu in this flow scale with Ra as $\overline{v}\propto\dot{m}\propto\mathrm{Ra}^{0.45}$ and $\mathrm{Nu}\propto\mathrm{Ra}^{0.9}$, respectively, in a wide range of $r=(\mathrm{Ra}-\mathrm{Ra}_{cr})/\mathrm{Ra}_{cr}$ variation. The ''normal'' scaling $\overline{v}\propto\sqrt{\mathrm{Ra}}$ is detected as $r\to 0$ and its range shrinks with decrease of the aspect ratio. The time evolution of the coherent flow is well described by the Landau amplitude equation with the appropriate selection of the Ra-dependent Landau constants. Analysis of the aspect ratio influence on the range of validity of anomalous scaling, observed in this paper, indicates the important role played by both thermal boundary conditions and geometry of the system.

DOI: 10.1103/PhysRevE.63.035304 PACS number(s): 47.27.Te, 47.11.+j, 47.20.Bp

Thermal convection in a Bénard cell is one of the classic, well-controlled systems, on which one can test the theoretical understanding of various natural phenomena like fluid instabilities, transition, strong turbulence itself, and the laws governing heat and mass transfer in turbulent flows. Originally, studies of high Ra-number turbulence in a convection cell were typically based on the idea that the temperature profile averaged over horizontal planes $\Theta(z)=\overline{T(x,y,z)}$ differs from an almost constant value only within thin thermal boundary layers of width δ_T. Then, assuming that the upper and lower boundary layers do not ''communicate,'' one obtains on dimensional grounds $\delta_T\propto\mathrm{Ra}^{-1/3}$ leading to the scaling of the dimensionless heat flux (Nusselt number, Nu) $\mathrm{Nu}\propto\mathrm{Ra}^{1/3}$. The Nusselt number is defined as the ratio of the total heat flux through the cell divided by the conductive heat flux for the same conditions. The accurate experiments on Bénard convection, using low-temperature helium, conducted by the Libchaber group, Heslot *et al.* [1], Castaing *et al.* [2], Wu [3], Belmonte *et al.* [4], showed that this relation is, in fact, incorrect and instead the Nusselt number at high enough Ra numbers scales as $\mathrm{Nu}\propto\mathrm{Ra}^{x}$ with $x\approx 0.285$, which is close to $x=2/7$. Recent data by Niemela *et al.* [5], show that $x\approx 0.3$ with possible logarithmic corrections. These experiments demonstrated the appearence of this scaling simultaneously with the onset of a powerful and persistent coherent large-scale flow (boundary layer ''wind'') with velocity $V\propto\mathrm{Ra}^{\xi}$ with $\xi\approx 0.48/0.49$ differing from the expected free-fall exponent $\xi=0.5$. The development of this large-scale flow in Bénard convection as well as in annular tanks was first reported in Howard and Krishnamurti [6].

To investigate the source and possible generality of the anomalous scaling of the convection-generated large-scale flow we conducted a numerical study of a system first considered by Welander [7] and Keller [8]. We are interested in the laminar large-scale flow generated as a result of a symmetry-breaking transition. This choice of system has one clear advantage: in the limit $r=(\mathrm{Ra}-\mathrm{Ra}_{cr})/\mathrm{Ra}_{cr}\to 0$, the mean velocity of the flow must obey the ''normal scaling'' $\overline{v}\propto\sqrt{r}$, and, as a consequence, the study of deviations from this scaling is much easier. Our motivation was prompted by the following qualitative argument. Assume that the flow in the bulk of a Bénard cell is simply a traditional Kolmogorov-like turbulence. We treat the flow as consisting of two parts: a viscous boundary layer of width δ_T and the bulk, where the effective transport coefficients are estimated as $\kappa\approx\nu\approx u_{rms}L=(u_{rms}L/\nu_0)\nu_0\approx\nu_o\,\mathrm{Re}$, where ν and κ are the effective viscosity and heat diffusivity (for Prandtl number, $\mathrm{Pr}\approx 1$), and ν_0 is the molecular viscosity. Thus, the bulk can be perceived as a very viscous (large mass) fluid. Setting, for the sake of the argument, $\nu\to\infty$ we conclude that the problem of stability of the thin boundary layer adjacent to the walls of the convection cell can be decoupled from the ''super-stable'' chaotic flow in the bulk. Thus, the qualitative picture of turbulence in a Bénard cell, presented above, combined with an idea that the low viscosity boundary layer is, in some respect, decoupled from the bulk makes the analogy with convection in a thin loop possible. However, if this analogy holds, it may explain the experimentally observed anomalous scaling. We investigate numerically the dynamics of the flow in two-dimensional cells $0\leqslant x,y\leqslant L$ with viscosity $\nu=\nu_0\neq\infty$ in the interval $0\leqslant|x|,|y|\leqslant\delta$, and $L-\delta\leqslant|x|,|y|\leqslant L$. Outside this interval, i.e., for $\delta<x,y<L-\delta$, $\nu=\infty$ meaning that $\mathbf{v}=0$.

In order to test the sensitivity of results to the geometry of the system, we have performed simulations in three configurations, corresponding to cells of different geometry. The first configuration is a cell of $L=1$ and $\delta/L=0.1$, the second is identical with the first, except for the aspect ratio $\delta/L=0.05$, whereas the third one corresponds to a circular geometry with the same diameter L and aspect ratio $\delta/L=0.1$; in the last case, the bottom fourth of the circumference of the circle is maintained at a high nondimensional temperature of 1, whereas the top fourth is kept at a low temperature of 0. The rest of the boundaries are considered to be adiabatic.

*Present address: CLT-F1, LVV-IET, Clausiusstrasse 33, Swiss Federal Institute of Technology (ETHZ), CH-8092, Switzerland. FAX: (+41-1) 632-1255.
Email address: ananias@lvv.iet.mavt.ethz.ch

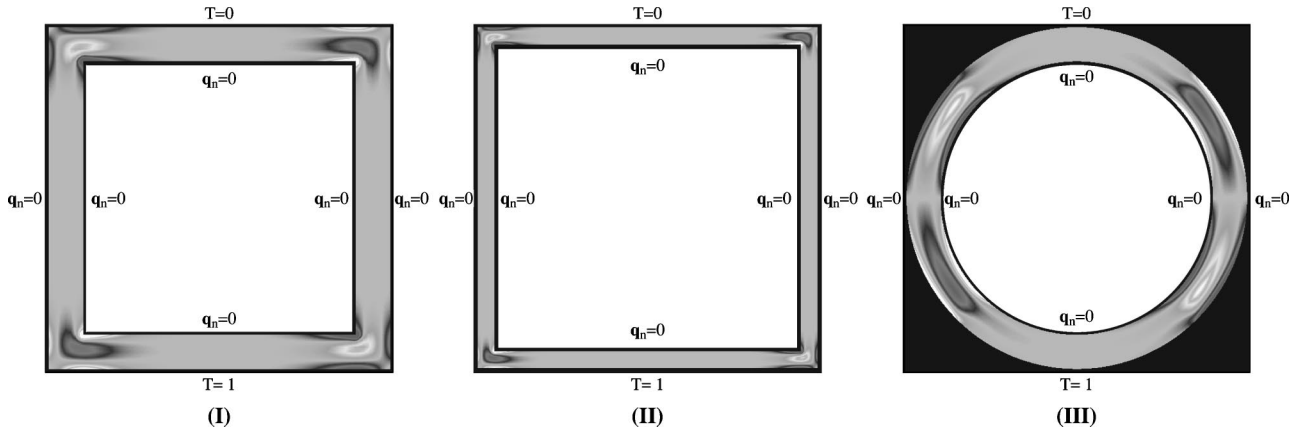

FIG. 1. Formation of convection rolls for the three configurations of the present paper, shown in terms of vorticity isocontours: (I) Ra=10 000, (II) Ra=100 000, and (III) Ra=30 000. Because this figure was generated by transformation of color plots to gray scale, the darkest tone does not correspond to the highest value.

Case III, which consists of a perfectly symmetric and nonsingular geometry, was investigated in order to verify that the somewhat unexpected results we found were not due to numerical errors, or due to numerical singularities (at corners). Here, we present some of the results obtained in two of the configurations (II and III), leaving a more detailed description for a future communication. The three convection cells and the boundary conditions used are shown in Figs. 1 configurations I–III.

The nondimensional equations of motion are the Boussinesq equations

$$\frac{\partial \mathbf{v}}{\partial t}+\mathbf{v}\cdot\boldsymbol{\nabla}\mathbf{v}=-\boldsymbol{\nabla}p+T+\frac{1}{\mathrm{Re}}\boldsymbol{\nabla}^2\mathbf{v},$$
$$\frac{\partial T}{\partial t}+\mathbf{v}\cdot\boldsymbol{\nabla}T=\frac{1}{\mathrm{Re\,Pr}}\boldsymbol{\nabla}^2T, \tag{1}$$

with $\boldsymbol{\nabla}\cdot\mathbf{v}=0$, where the nondimensionalizing velocity scale is $U=\nu/L\ \mathrm{Gr}^{1/2}$ and $\mathrm{Re}=\mathrm{Gr}^{1/2}$, where Gr is the Grasshof number (here, Ra=Gr since Pr=1). For given geometry, the only nondimensional system parameter is the Rayleigh number, $\mathrm{Ra}=\beta g\Delta TL^3/\kappa\nu$, where β is the thermal expansion coefficient of the fluid, κ is the heat conductivity, and ν is its kinematic viscosity.

For the time integration of Eqs. (1), we use a fractional step method, in conjunction with a mixed explicit/implicit stiffly stable scheme of second order of accuracy in time, Karniadakis *et al.* [9]. A consistent Neumann boundary condition is used for the pressure, based on the rotational form of the viscous term, which nearly eliminates splitting errors at solid (Dirichlet) velocity boundaries, Tomboulides *et al.* [10]. The spatial discretization of the resulting Helmholtz equations is performed using two-dimensional Legendre spectral elements, Patera [11]. The resulting matrices for the numerical solution of the two-dimensional Helmholtz equations are solved using preconditioned conjugate gradient iterative solvers. The resolution can be increased by increasing either the number of elements or the order of the interpolants inside each element. In the simulations presented here, the resolution was improved mainly by increasing the order of interpolants. Several resolution tests, not reported here, were performed and a typical discretization consists of 40 elements with up to 15 points in each direction per element. The collocation points are clustered near the boundaries, where a higher resolution is necessary. In general, because of the laminar nature of the flow in the range of Ra numbers investigated, the computational cost was not a limiting factor; a typical simulation took a few hours on a SGI/R10000 workstation. The resolution became limiting only in the simulation of very high Ra cases (over 10^{10} or so).

At very low Rayleigh numbers, the fluid inside the cell is not in motion. As Ra increases over Ra'_{cr}, the first transition, corresponding to the appearance of convection rolls, occurs. Here, because of the geometry, convection rolls at scale $l\approx\delta$ appear only at the corners of the domain, and display a double-flip symmetry with respect to the diagonal. Isocontours of vorticity, consisting of counter-rotating vortices located at the four corners, for $\mathrm{Ra}'_{cr}\leqslant\mathrm{Ra}\leqslant\mathrm{Ra}_{cr}$ (Ra_{cr} corresponding to the second transition), are shown in Figs. 1 configurations I–III.

As the Ra number increases over Ra_{cr}, a symmetry-breaking occurs, resulting in the appearance of a large-scale mean flow. This transition is a linear one and corresponds to a regular bifurcation (or exchange of stability) where the resulting flow is not time dependent (i.e., the crossing eigenvalue has zero frequency). The average mass flux ($\dot{m}$) and nondimensionalized heat flux (Nu) for case II are plotted in Figs. 2(a) and 2(b), respectively, as functions of $\log(r)$. The value of Ra_{cr} for case II was found to be $\mathrm{Ra}_{cr}=114\,648$. As can be observed for case II, the mass flux scales approximately as $\dot{m}\propto r^{0.45}$, and the Nu scales as $\mathrm{Nu}\propto r^{0.9}$ for r between 0.01 and approximately 100. The bottom part of Figs. 2(a) and 2(b) shows $\dot{m}$ multiplied by $r^{-0.45}$ and (Nu−1) multiplied by $r^{-0.9}$, respectively. Unlike case II, in the other two configurations (I and III) a scaling of $\dot{m}\propto r^{0.5}$ was detected very close to Ra_{cr} (for $r<0.1$) with a transition to the $r^{0.45}$ scaling after that.

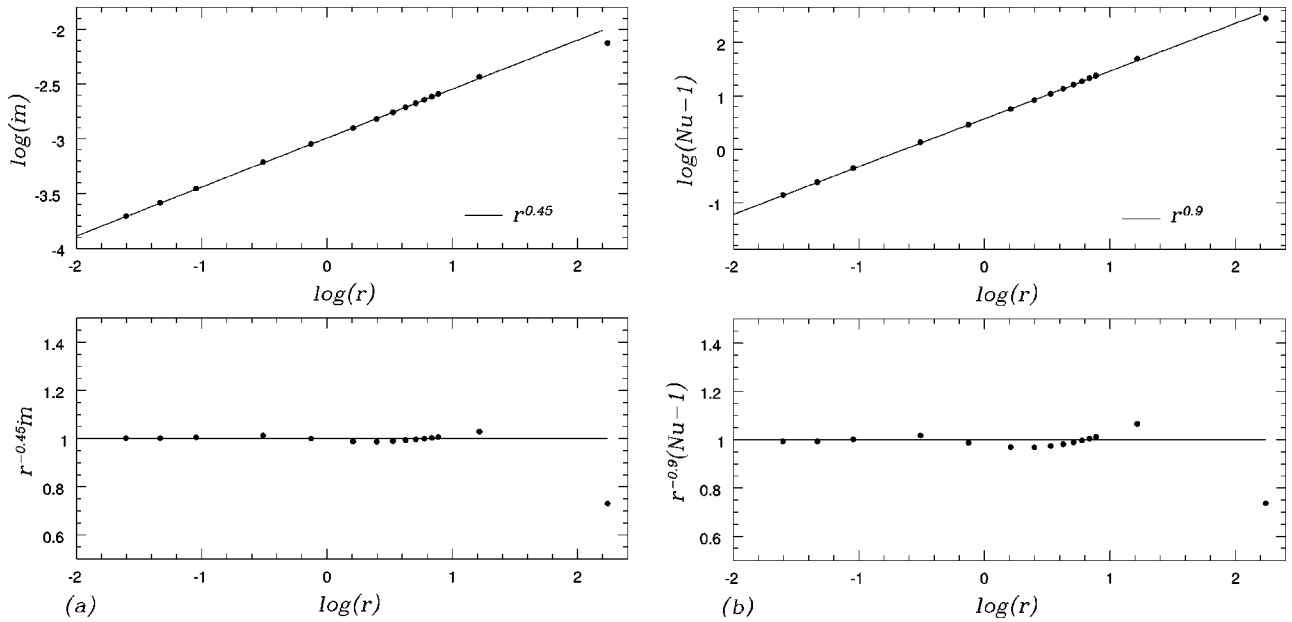

FIG. 2. (a) (Top) Logarithmic plot of the large-scale average mass flux, $\dot{m}$, as function of $\log(r)$, for case II; (bottom) $r^{-0.45}\dot{m}$ as function of $\log(r)$. (b) (Top) Logarithmic plot of the Nusselt number Nu as function of $\log(r)$, for case II; (bottom) $r^{-0.45}(\mathrm{Nu}-1)$ as function of $\log(r)$. The base of the logarithm is 10.

The amplitude of the large-scale mean flow, which is generated after the second transition at $\mathrm{Ra}=\mathrm{Ra}_{cr}$, increases with Ra and its kinetic energy averaged over the domain was used in the Landau amplitude equation to model this transition. This kinetic energy, A^2, is governed by the amplitude equation $dA^2/dt=\gamma A^2-\alpha A^4$ (Landau and Lifshitz [12]). The solution to this equation is given by the following expression

$$A^2(t)=\gamma[(\gamma-\alpha A_0^2)e^{-\gamma(t-t_0)}/A_0^2+\alpha]^{-1}, \qquad (2)$$

where γ and α are the so-called Landau constants, and $A_0=A(t_0)$. We found that our results can accurately be modeled using this equation for a wide range of Ra numbers, $10^{-2}\leqslant r\leqslant 10^{2}$. An example of a typical comparison between numerical results and Eq. (2) for this range of r is shown in Figs. 3(a) and 3(b), corresponding to case III for $r=0.16$ (Ra_{cr} for this case is equal to 34 417). These figures show the computed total kinetic energy of the flow, shown with solid line, and $A^2(t)$ from Eq. (2), shown with dotted line, and as can be observed from the figure the difference is

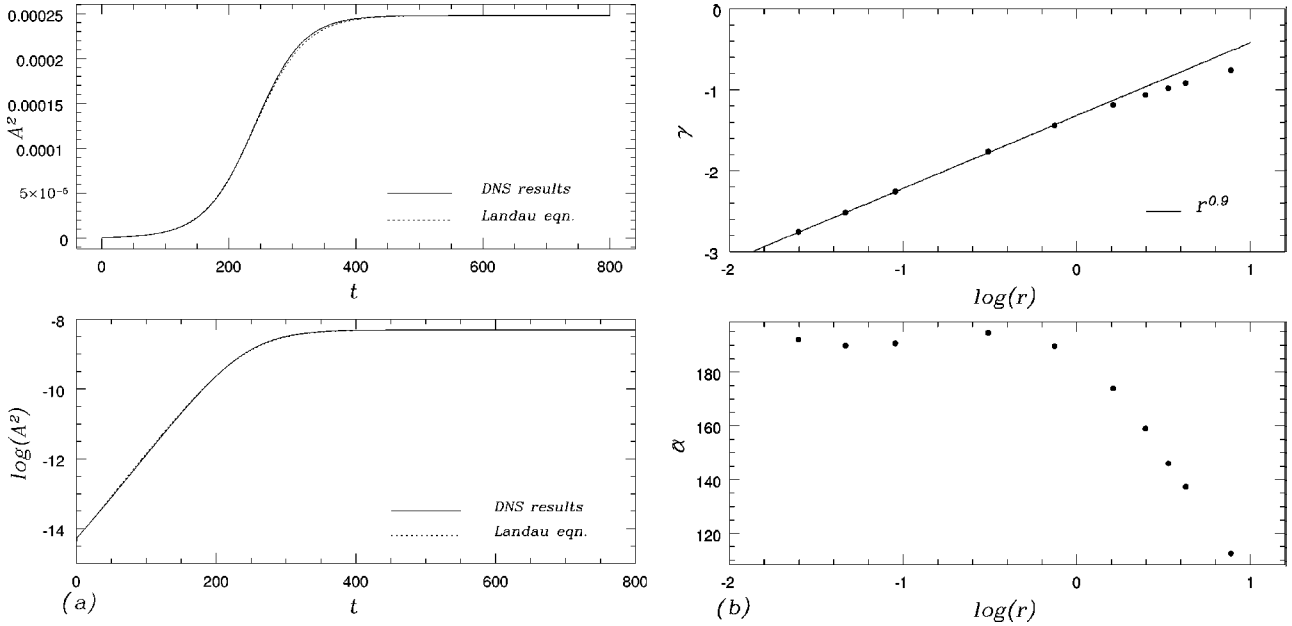

FIG. 3. (a) Comparison between the numerical simulation and Eq. (2) for case III, $r=0.16$. (b) Logarithmic plot of the Landau constants γ and α as functions of r in the large-scale flow regime ($\mathrm{Ra}>\mathrm{Ra}_{cr}$), for case II. The base of the logarithm is 10.

almost negligible. It is clear from the expression for $A^2(t)$ that at steady state A is given by $A=\sqrt{\gamma/\alpha}$. The Landau constants γ and α were calculated from numerical simulation results and are shown in Figs. 3(c) and 3(d), for case II. Figures 3(c) and 3(d) suggest that for case II $\gamma \propto r^{0.9}$ up to r of about 1 or so. The second exponent α was found to be very close to 190 for all r up to 1 and to decrease monotonically for higher r. For the other two cases a transition was observed in the behavior of γ at $r=0.1$ from a $\gamma \propto r^1$ to a $\gamma \propto r^{0.9}$ scaling. The fact that $\overline{v} \approx A \propto r^{0.45}$ in a wide interval where strong deviations of both γ and α from a simple scaling [see Figs. 3(c) and 3(d)] are observed, is somewhat surprising.

For values of r lower than a certain level depending on aspect ratio (10 for $\delta/L=0.1$ and 100 or even higher for $\delta/L=0.05$), the system dynamics is very well captured by the amplitude equation. For higher magnitudes of r one can clearly observe the appearance of other modes, which are oscillatory and, although damped at long times, do appear in the initial transients. These modes lead to instabilities at higher Ra numbers (e.g., higher than 10^8 for case I) and after that the flow becomes time dependent.

In summary, in the simple system we considered here, which can mimic the experimentally observed large-scale flow generation in Bénard convection, first an instability occurs at $\mathrm{Ra}=\mathrm{Ra}'_{cr}$, leading to a symmetric steady flow pattern. After the symmetry-breaking, at $\mathrm{Ra}=\mathrm{Ra}_{cr}$, the observed $\overline{v} \propto \dot{m} \propto \mathrm{Ra}^{0.45}$ and $\mathrm{Nu} \propto \mathrm{Ra}^{0.9}$. The onset of this anomalous scaling is correlated with the simultaneous modification of the Rayleigh number dependence of the coefficients in the Landau amplitude equation, accurately describing the data in a wide range of r. The fact that the results obtained in this paper are so well described by the Landau equation may be explained as follows; due to the restricting geometry, the dynamics are well represented by a small number of modes even when Ra is relatively large. The more surprising outcome in the present paper is the anomalous scaling $\overline{v}(r) \propto r^{0.45}$, observed in the entire investigated interval $10^{-2}<r<10^2$ in the low aspect ratio cell (case II). Actually, the width of the interval increased with decrease of the aspect ratio. At present, we do not understand the origins of this effect. However, all tests, conducted in the course of this paper, indicated that the effect is due to a complicated interaction between geometry and thermal boundary conditions, breaking all geometrical symmetries of the system. In fact, when artificially changing the nature of the problem from natural convection to a forced convection for case III, by solving only for the momentum equation with a steady forcing term in the azimuthal direction (simulating the role of a thermal driving force), and thus maintaining the geometrical symmetry of the system and still in the presence of a large-scale flow, the mass flux scaled linearly with the amplitude of the force; no anomalous scaling was observed for this case. We believe, this is the main difference between convection processes in finite and infinite cells, in which the imposition of the thermal boundary conditions does not impose any symmetry breaking.

We are grateful to W. Malkus and E. Spiegel for bringing Refs. [7,8] to our attention.

[1] F. Heslot, B. Castaing, and A. Libchaber, Phys. Rev. A **36**, 5870 (1987).

[2] B. Castaing, G. Gunaratne, F. Heslot, L. Kadanoff, A. Libchaber, S. Thomae, X. Z. Wu, S. Zaleski, and G. Zanetti, J. Fluid Mech. **204**, 1 (1989).

[3] X. Z. Wu, Ph.D. dissertation, The University of Chicago, 1991 (unpublished).

[4] A. Belmonte, A. Tilgner, and A. Libchaber, Phys. Rev. E **50**, 269 (1994).

[5] J. J. Niemela, L. Skrbek, K. R. Sreenivasan, and R. J. Donnely, Nature (London) **434**, 837 (2000).

[6] R. Krishnamurti and L. N. Howard, Proc. Natl. Acad. Sci. USA **78**, 1981 (1981).

[7] P. Welander, J. Fluid Mech. **29**, 17 (1967).

[8] J. B. Keller, J. Fluid Mech. **29**, 599 (1967).

[9] G. E. Karniadakis, M. Israeli, and S. A. Orszag, J. Comput. Phys. **97**, 414 (1991).

[10] A. G. Tomboulides, M. Israeli, and G. E. Karniadakis, J. Sci. Comput. **4**, 291 (1989).

[11] A. T. Patera, J. Comput. Phys. **54**, 468 (1984).

[12] L. D. Landau and E. M. Lifshitz, *Fluid Mechanics*, 2nd ed. (Pergamon, Oxford, 1987).